JOURNAL OF VIROLOGY, Jan. 2001, p. 469–479 Vol. 75, No. 1
0022-538X/01/$04.00+0 DOI: 10.1128/JVI.75.1.469–479.2001

Induction and Inhibition of Apoptosis by Pseudorabies Virus in the Trigeminal Ganglion during Acute Infection of Swine

NURIA ALEMAÑ,[1]* MARÍA ISABEL QUIROGA,[2] MÓNICA LÓPEZ-PEÑA,[2] SONIA VÁZQUEZ,[2] FLORENTINA H. GUERRERO,[1] AND JOSÉ M. NIETO[2]

Departamento de Anatomía y Producción Animal[1] and Departamento de Patología Animal (Anatomía Patológica),[2] Facultad de Veterinaria, Universidad de Santiago de Compostela, 27002 Lugo, Spain

Received 29 June 2000/Accepted 9 October 2000

We examined the ability of pseudorabies virus (PRV) to induce and suppress apoptosis in the trigeminal ganglion during acute infection of its natural host. Eight pigs were intranasally inoculated with a virulent field strain of PRV, and at various early times after inoculation, the trigeminal ganglia were assessed histologically. PRV-infected cells were detected by use of immunohistochemistry and in situ hybridization, and apoptosis was identified by in situ terminal deoxynucleotidyltransferase-mediated dUTP nick end labeling. Light and electron microscopy was also used for morphological studies. Apoptosis was readily detected among infiltrating immune cells that were located surrounding PRV-infected neurons. The majority of PRV-infected neurons did not show morphological or histochemical evidence of apoptosis, even including those neurons that were surrounded by numerous inflammatory cells and exhibited profound pathological changes. However, neuronal virus-induced apoptosis also occurred but at a sporadic low level. These findings suggest that PRV is able to block apoptosis of infected trigeminal ganglionic neurons during acute infection of swine. Furthermore, our results also suggest that apoptosis of infiltrating inflammatory cells may represent an important viral mechanism of immune evasion.

Suid herpesvirus 1, usually named pseudorabies virus (PRV) or Aujeszky's disease virus, is a member of the subfamily *Alphaherpesvirinae*, which causes a disease with a worldwide distribution in swine. PRV is a highly neurotropic virus and after primary replication in the nasopharyngeal mucosa invades the central nervous system (CNS) through several nervous pathways. Infection of the CNS by PRV produces a nonsuppurative meningoencephalitis that is often fatal in piglets (6, 10, 26). Older animals can survive the infection, although they may develop respiratory disorders induced by PRV replication in the respiratory tract, and abortion can occur in pregnant sows due to the occurrence of viremia (18, 27). Like other herpesviruses, PRV establishes a lifelong latent infection in neuronal and nonneuronal cells of its host. Such quiescent infection may be reactivated, and PRV can spread to other susceptible animals (11, 23).

It has been shown that viral infection is a powerful stimulus that triggers the biochemical machinery of suicide or apoptosis of infected cells. In this context, many viruses have acquired their own antiapoptotic genes, which can block or delay death of infected cells and so maximize the production of viral progeny (32, 39, 41). Among them, human herpes simplex virus type 1 (HSV-1) and HSV-2 and bovine herpesvirus 1 (BHV-1), alphaherpesviruses that share a number of biological properties with PRV, have developed specific strategies to interfere with the host cells' apoptotic pathway, not only to prevent premature death of the cell but also to establish persistent infections. A number of gene products have been reported to render infected cells resistant to apoptosis induced by HSV-1 itself, as well as by other known inducers (reviewed in reference 2). In this way, it was shown that the Us3 (21, 25), Us5 (21), ICP27 (1), ICP22 (2), and latency-associated transcript (LAT) (34) genes of HSV-1 play a role in preventing the apoptosis of infected cells. For HSV-2 also, the Us3 gene was shown to have antiapoptotic activity (15). In the case of BHV-1, the LATs also appear to promote the survival of infected neurons by suppressing apoptosis (8). It has not been demonstrated to date whether PRV encodes products with such antiapoptotic function.

On the other hand, alphaherpesviruses are specialists in evading the host defense mechanisms. It is becoming increasingly clear that this ability depends, at least in part, on the virus's capability for controlling the signaling and molecular events of the apoptotic pathway. On that score, it has been demonstrated that HSV-1 protects infected nonlymphoid cells from cytotoxic T-lymphocyte-induced apoptosis (20) and that both HSV-1 (19, 35, 38) and BHV-1 (12, 14, 44) can infect activated $CD4^+$ T lymphocytes, leading to apoptosis of these cells and the suppression of cell-mediated immunity. Regarding PRV, several authors have focused on the interactions between this virus and peripheral blood mononuclear cells. The occurrence of cell-associated viremia after experimental infection of pigs has been reported (4, 29, 33), and both in vivo and in vitro studies have shown that monocytes are the porcine mononuclear cells most susceptible to PRV infection, followed by stimulated T lymphocytes (7, 28, 29, 43). Although some monocytes and T lymphocytes die due to infection after an in vitro inoculation with PRV (7, 43), it has not been established whether it occurs through an apoptotic pathway and, if so, what could be the role of immune cell apoptosis in PRV pathogenesis during productive infection of swine.

* Corresponding author. Mailing address: Departamento de Anatomía, Facultad de Veterinaria, Campus Universitario de Lugo, 27002 Lugo, Spain. Phone: 34 982 252231. Fax: 34 982 252195. E-mail: nalemany@lugo.usc.es.

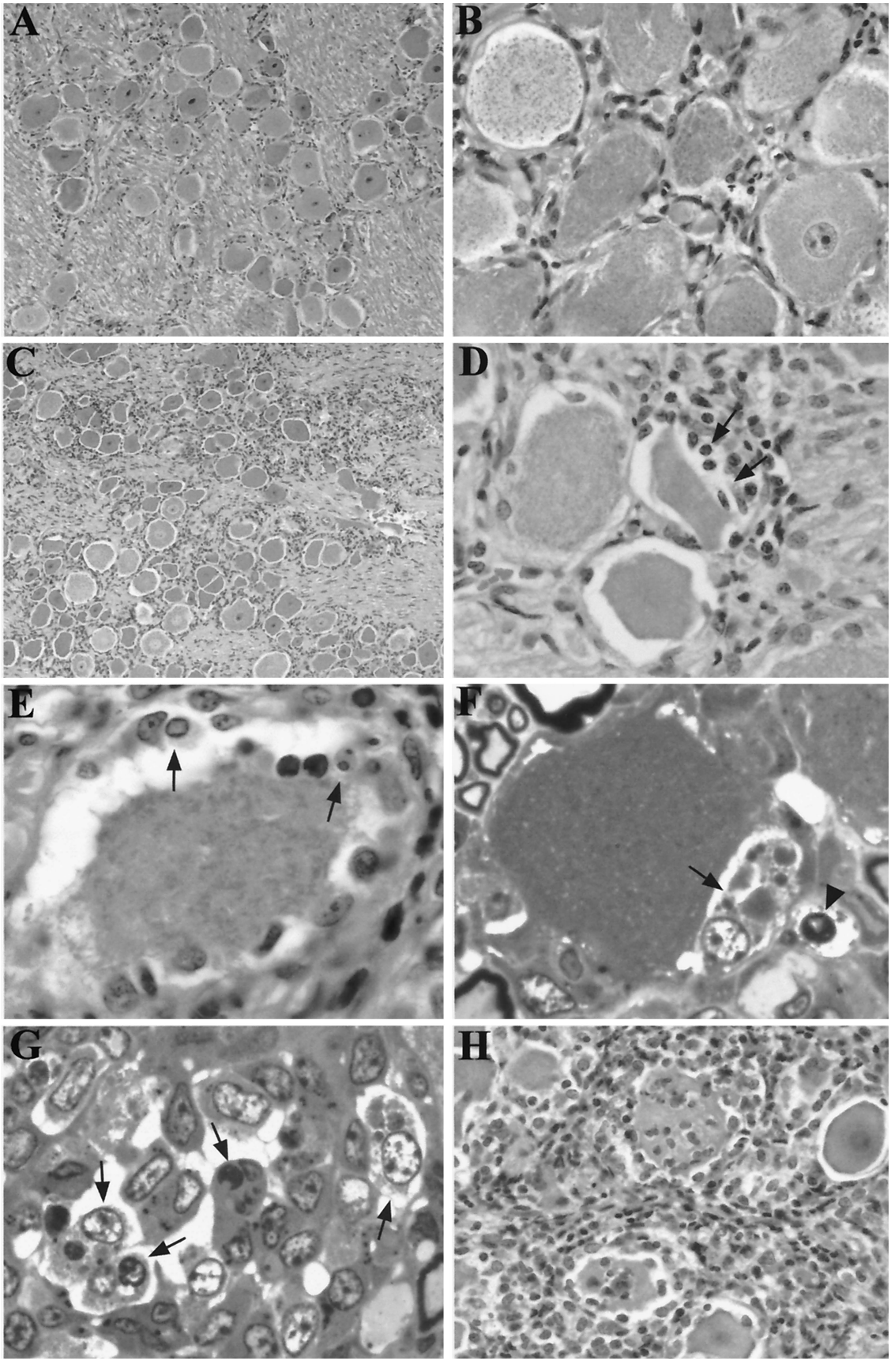
A
B
C
D
E
F
G
H

In this study, a virulent strain of PRV was used to determine whether this virus induces and/or blocks apoptosis in the trigeminal ganglion (TG) during acute infection of its host. The TG was preferred because the trigeminal nervous pathway is usually involved in the invasion of the CNS by PRV during natural infection of swine and because TG neurons are the most common site where the virus persists in a latent state. Our study shows that the majority of PRV-infected TG neurons are resistant to apoptosis induced by the virus itself as well as by cytotoxic immune cells. Moreover, our results also suggest that apoptosis of infiltrating inflammatory cells may be an important viral mechanism of immune evasion.

MATERIALS AND METHODS

Animals and virus. A total of nine 2-month-old conventional pigs that were not vaccinated against PRV and were seronegative for PRV was used in this study. They were caged individually under strict isolation containment, fed with commercial food, and carefully monitored during the experiment. Eight pigs were infected intranasally with a virulent strain of PRV isolated in northwestern Spain (INIA reference no. E-974) from brain tissue of naturally infected pigs and adapted to cell culture according to the method described by Puentes et al. (36). Each inoculated animal was given 2 ml of suspension containing $10^{6.5}$ 50% tissue culture infective doses of PRV per ml, 1 ml per nostril. Pigs were euthanized at 12, 24, 48, and 72 h postinfection (hpi), two animals at each time point. The remaining uninfected pig was killed at the beginning of the experiment and served as a negative control. At necropsy, the TG were removed, fixed in 10% buffered formalin, processed by routine histological methods, and embedded in paraffin. Small pieces from TG obtained from animals killed at 48 and 72 hpi were also placed in cold 2.5% buffered glutaraldehyde, postfixed in 1% aqueous osmium tetroxide, dehydrated in ethanol solutions, and embedded in Epon 812.

Light microscopy. For light microscopy observations, paraffin-embedded TG samples were sectioned at 4 μm and stained with hematoxylin and eosin (HE). Semithin sections (0.5 to 1.0 μm) were also obtained from Epon 812 blocks and stained with toluidine blue (TB).

Immunohistochemistry (IHC). TG sections were deparaffinized, rehydrated, and incubated with 0.3% H_2O_2 in phosphate-buffered saline (PBS) (pH 7.4) for 45 min at room temperature (RT) to inactivate endogenous peroxidase. PRV antigen detection was performed by using a rabbit polyclonal antiserum and the large-volume DAKO LSAB kit peroxidase (Dako Corp., Carpinteria, Calif.) according to the manufacturer's instructions. Finally, the slides were developed by incubation with freshly prepared 0.05% diaminobenzidine and 0.3% H_2O_2 in PBS, rinsed with distilled water, counterstained with hematoxylin, and coverslipped. In each series of stained sections, positive and negative controls were included to assess the specificity of the assay. Sections of TG from pigs intranasally infected with strain E-974 in a previous experiment (unpublished data) were used as positive controls for staining for PRV antigen. Negative control slides were TG sections from the uninfected animal.

In situ hybridization (ISH). PRV DNA was detected on paraffin sections as previously described (37) with some modifications. Sections were deparaffinized, rehydrated, and deproteinized with 0.2 N HCl for 20 min at RT. After a washing in distilled water, sections were treated with 20 μg of proteinase K (Sigma)/ml in PBS at 37°C for 20 min. Slides were rinsed in PBS and postfixed in fresh 4% paraformaldehyde in PBS for 5 min. Acetylation was performed to reduce the nonspecific binding of the probe to other reactive groups in 0.1 M triethanolamine (pH 8.0). After 5 min of incubation at RT, 0.25% acetic anhydride was added for an additional 5 min and then sections were rinsed in distilled water. Sections were denatured in 60% deionized formamide in 0.1× standard saline citrate (SSC) (1× SSC is 150 M NaCl plus 15 M sodium citrate [pH 7.0]) for 15 min at 65°C, washed in cold 0.1× SSC, and dehydrated. TG sections were incubated in the hybridization mixture containing 50% deionized formamide, 4× SSC, 10% dextran sulfate, 1% Denhardt's solution (0.02% Ficoll, 0.02% polyvinylpyrrolidone, 0.02% bovine serum albumin), 500 μg of salmon testis DNA/ml, and 0.1 ng of labeled probe/ml. The DNA probe specific for PRV was the *Bam*HI-7 fragment of the PRV genome cloned in plasmid pBR325 and labeled by the method of random-primed labeling with digoxigenin-11-dUTP using a commercial kit (DIG DNA labeling and detection kit; Boehringer Mannheim Corp., Indianapolis, Ind.). The hybridization was carried out overnight at 42°C. After hybridization, slides were washed twice in 4× SSC for 5 min at RT, once in 2× SSC for 10 min at 37°C, once in 0.2× SSC containing 60% formamide for 10 min at 37°C, twice in 2× SSC for 5 min at RT, twice in 0.2× SSC for 5 min at RT, and once in buffer I (100 mM maleic acid, 150 mM NaCl [pH 7.5]) for 5 min at RT. The anti-digoxigenin-alkaline phosphatase conjugate (Boehringer Mannheim) was diluted 1:400 in buffer II (1% blocking reagent in buffer I; Boehringer Mannheim) and then added to the tissue sections. Incubation was carried out in a humidified chamber for 1 h at RT. Slides were washed twice in buffer I for 5 min each and once in buffer III (100 mM Tris-HCl, 100 mM NaCl, 50 mM $MgCl_2$ [pH 9.5]) for 5 min at RT. Finally, slides were incubated in the dark with the color substrate solution consisting of 4-nitroblue tetrazolium chloride (Boehringer Mannheim) and 5-bromo-4-chloro-3-indolylphosphate (X-phosphate; Boehringer Mannheim) in buffer III. The color reaction was stopped in TE buffer (10 mM Tris-HCl, 1 mM EDTA [pH 8.0]). Slides were counterstained with 1% methyl green, washed with distilled water, air dried, and coverslipped before microscopic observation. Positive and negative controls (described above) were always performed simultaneously with the tested slides.

In situ detection of apoptosis. TG sections were deparaffinized, rehydrated, permeabilized by incubation in 20-μg/ml proteinase K in PBS for 20 min at 37°C, and washed twice for 5 min in PBS. The terminal deoxynucleotidyltransferase-mediated dUTP nick end labeling (TUNEL) method was used for the histochemical detection of apoptotic cells. The cells were detected with a kit which utilizes alkaline phosphatase (In Situ Cell Death Detection kit, AP; Boehringer Mannheim); it was used following the manufacturer's directions. The color reaction was developed and slides were counterstained as previously described in the ISH protocol. Negative controls were always included in each series of sections assayed.

Double labeling. IHC tests combined with the TUNEL method were also performed on single sections. Slides which had been assayed by TUNEL were washed in PBS, and then IHC tests were done as described earlier.

Transmission electron microscopy. For ultrastructural examinations, ultrathin sections were obtained from Epon 812 blocks, counterstained with uranyl acetate and lead citrate, and examined under a JEOL SX100 transmission electron microscope.

RESULTS

Light microscopy examination. As expected, the magnitude of pathology induced by PRV infection in the TG correlated with the advancing survival time of the infected animals. In comparison with uninfected TG (Fig. 1A and B), a few mononuclear cells, mainly lymphocytes and macrophages according to their morphological characteristics, were already present in scattered areas of the TG at 12 hpi (Fig. 1C). These cells were localized near blood vessels and around satellite cells, and

FIG. 1. Morphological findings in the TG from uninfected and PRV-infected pigs. (A and B) Sections of TG obtained from the uninfected pig and stained with HE. Both panels show the normal histological structure of this organ. (C and D) Sections of TG stained with HE at 12 hpi. (C) A small number of mononuclear inflammatory cells (upper portion of the field) was already present in the TG. (D) Lymphocytes and macrophages (arrows) were observed in direct apposition to neurons showing pathological changes. (E and F) Sections of TG stained with HE and TB, respectively, at 48 hpi. (E) Apoptotic cells (arrows) among perineuronal inflammatory cells. (F) A macrophage containing phagocytosed apoptotic bodies (arrow) between a neuron and its ensheathing satellite cell. An apoptotic lymphocyte can also be observed (arrowhead). (G and H) Sections of TG stained with TB and HE, respectively, at 72 hpi. (G) Numerous apoptotic bodies (arrows) free or phagocytosed by macrophages within a focus of neuronophagia. (H) Neurons, even those exhibiting profound pathological changes, did not show morphological features of apoptosis. All light microscopy images in this report were obtained with a digital camera (Olympus DP10) adapted to a photomicroscope (Olympus BX50). The software used to modify brightness and contrast was Adobe Photoshop 4.0 for Windows. Original magnifications, ×100 (A and C), ×200 (H), ×400 (B and D), and ×1,000 (E, F, and G).

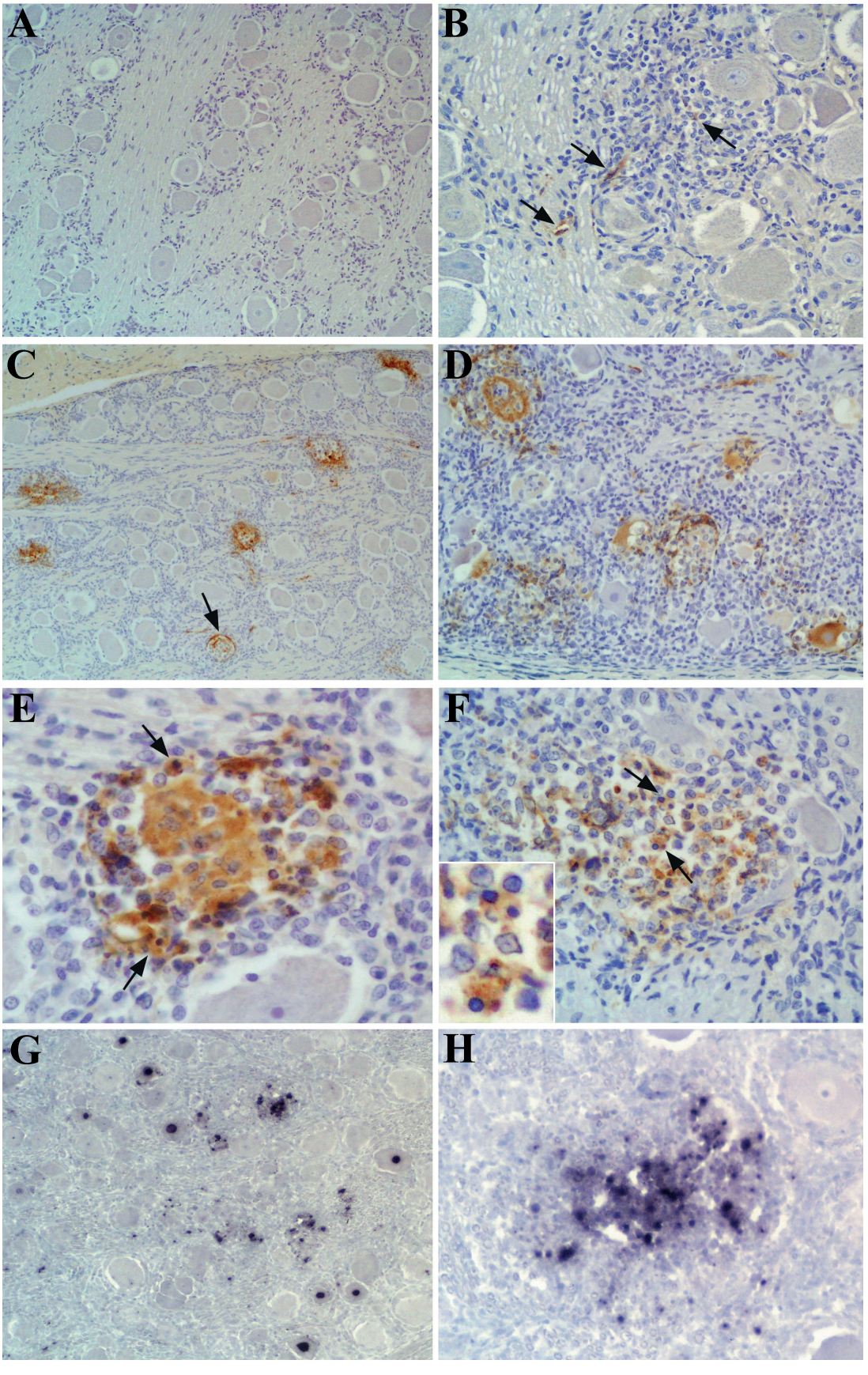
A
B
C
D
E
F
G
H

some were seen in direct apposition to neurons (Fig. 1D). Pathological changes became apparent at 24 hpi. Large numbers of mononuclear cells infiltrated specific areas of the TG and caused small foci of infection, which contained sensory neurons exhibiting hallmarks of viral infection. The extent of infection was greatly increased at 48 hpi. Several neurons at different stages of neuronophagia were readily found within multiple foci of inflammation. It was noteworthy that individual, infiltrating immune cells showed distinctive morphological features of apoptosis, such as cell shrinkage, nuclear fragmentation, and apoptotic body formation (Fig. 1E). Apoptotic bodies were also identified as having been phagocytosed by macrophages (Fig. 1F). Many of the apoptotic cells in these sections could be identified as lymphocytes by morphological criteria, but a few macrophages also had nuclei exhibiting typical hallmarks of apoptosis, including condensation of chromatin at the nuclear margin. At 72 hpi, the number of infiltrating immune cells in the TG was substantially larger, as was the number of neurons involved in the extensive inflammatory reaction. Apoptosis of infiltrating inflammatory cells was prevalent in the numerous foci of neuronophagia (Fig. 1G). Although many sensory neurons appeared shrunken and exhibited irregular outlines of both the nucleus and cytoplasm, typical features of apoptosis were not observed in this ganglionic cell type at any time investigated (Fig. 1H).

IHC. No virus antigen was detected at 12 hpi or in TG sections from the uninfected pig (Fig. 2A). PRV antigen was first detected in the cytoplasm of very few infiltrating lymphocytes and macrophages at 24 hpi (Fig. 2B). No positive neuronal immunoreaction was observed at this time of infection. At 48 hpi, viral antigen was present in the cytoplasm of isolated sensory neurons of the TG, as well as in surrounding inflammatory cells (Fig. 2C). Many of the immunolabeled neurons were encircled by antigen-positive satellite cells (Fig. 2C), and positive cells, which by their distribution and morphology appeared to be fibroblasts and Schwann cells, were also observed. The number of immunolabeled neurons, lymphocytes, and macrophages increased at 72 hpi (Fig. 2D). Positive immunoreaction was also detected in both free and phagocytosed apoptotic cells within foci of inflammation at both 48 and 72 hpi (Fig. 2E and F). Although PRV antigen was detected in cells distributed in areas of the TG that exhibited severe inflammatory lesions, there was in general a poor correlation between the number of immunolabeled cells and the magnitude of pathological changes.

ISH. ISH was performed on TG sections which were immediately adjacent to those tested for IHC to corroborate the presence of PRV DNA in neurons and infiltrating inflammatory cells. TG sections obtained from the noninoculated pig and from pigs killed at 12 hpi were uniformly negative. At 24 hpi, PRV DNA was detected in the nuclei of very few sensory neurons and also in the nuclei of a small number of infiltrating immune cells. Infected neurons were localized mainly in an isolated fashion at 48 hpi (Fig. 2G), but at 72 hpi they appeared clustered in groups of positive cells. Lymphocytes and macrophages around infected neurons and within foci of neuronophagia usually showed a positive reaction to the ISH technique (Fig. 2G and H). Viral DNA was also detected in the nuclei of satellite cells.

In situ TUNEL. To confirm the occurrence of apoptosis in infiltrating inflammatory cells, the TUNEL technique was performed on TG sections. None of the sections obtained from animals killed at 12 hpi (Fig. 3A) or from the uninfected control contained TUNEL-positive cells. At 24 hpi, small numbers of TUNEL-positive cells were detected in focal areas of the TG (Fig. 3B). At 48 hpi, increasing numbers of TUNEL-positive cells were localized around neurons and within foci of neuronophagia. The TUNEL-positive cells were significantly more abundant at 72 hpi (Fig. 3C), and many of them could be observed within the cytoplasm of cells, which indicates engulfment of apoptotic cells by neighboring cells and macrophages (Fig. 3D). Apart from the fact that the TUNEL assay detected apoptotic cells earlier, at 24 hpi, the distribution and temporal development of TUNEL-positive cells in the TG of infected pigs correlated directly with the distribution and temporal development of apoptotic immune cells noted previously on sections stained for pathological examination. A TUNEL-positive signal was not detected in the nuclei of sensory neurons, even in those cells showing prominent pathological changes (Fig. 3B to D).

Double labeling. Double-labeling experiments confirmed that PRV antigen-positive cells and apoptotic cells were concentrated in the same regions of the TG in conjunction with extensive tissue damage (Fig. 3E). It was surprising to find double-labeled neurons in the TG of one animal killed at 48 hpi. This phenotype was uncommon, since it was not detected in previously performed TUNEL assays, and only a total of 3 out of approximately 30 PRV antigen-positive neurons with visible nuclei displayed TUNEL staining at this time postinfection (Fig. 3E). Double-positive neurons exhibited a well-preserved morphology, and associated inflammatory reaction was lower than in IHC-positive–TUNEL-negative neurons (Fig. 3E and F). However, a few immune cells were also seen in direct contact with apoptotic neuron cell bodies (Fig. 3E). Double-positive neurons also exhibited lighter staining of PRV antigen than did infected, nonapoptotic cells (Fig. 3E). A mixture of single- and double-labeled infiltrating inflammatory cells was observed surrounding all PRV-infected neurons (Fig. 3F). Although it was difficult to distinguish individual cells accurately, the majority of them appeared to be single labeled

FIG. 2. Detection of PRV antigen (A to F) by IHC and of PRV DNA (G and H) by ISH in the TG of uninfected and PRV-infected pigs. (A) TG section from the uninfected pig showing no positive immunoreaction. (B) Viral antigen (brown stain) was detected in the cytoplasm of a small number of infiltrating immune cells (arrows) at 24 hpi. (C) At 48 hpi, PRV antigen was present in scattered neurons, in perineuronal inflammatory cells, and in satellite cells (arrow). (D) Multiple foci of inflammation containing PRV antigen-positive neurons and inflammatory cells at 72 hpi. (E) A PRV-infected neuron in the process of being eliminated by immune cells at 48 hpi. Note the presence of viral antigen in inflammatory cells, some of them showing apoptotic morphology (arrows). (F) At 72 hpi, an infected neuron has been degraded and viral antigen is present in many inflammatory cells, some of them exhibiting clearly an apoptotic appearance (arrows and inset). (G) PRV DNA (black stain) was detected in the nuclei of neurons and in infiltrating inflammatory cells at 48 hpi. (H) Focus of neuronophagia containing numerous PRV-infected inflammatory cells at 72 hpi. Original magnifications, ×100 (A, C, D, and G), ×200 (B and H), and ×400 (E and F).

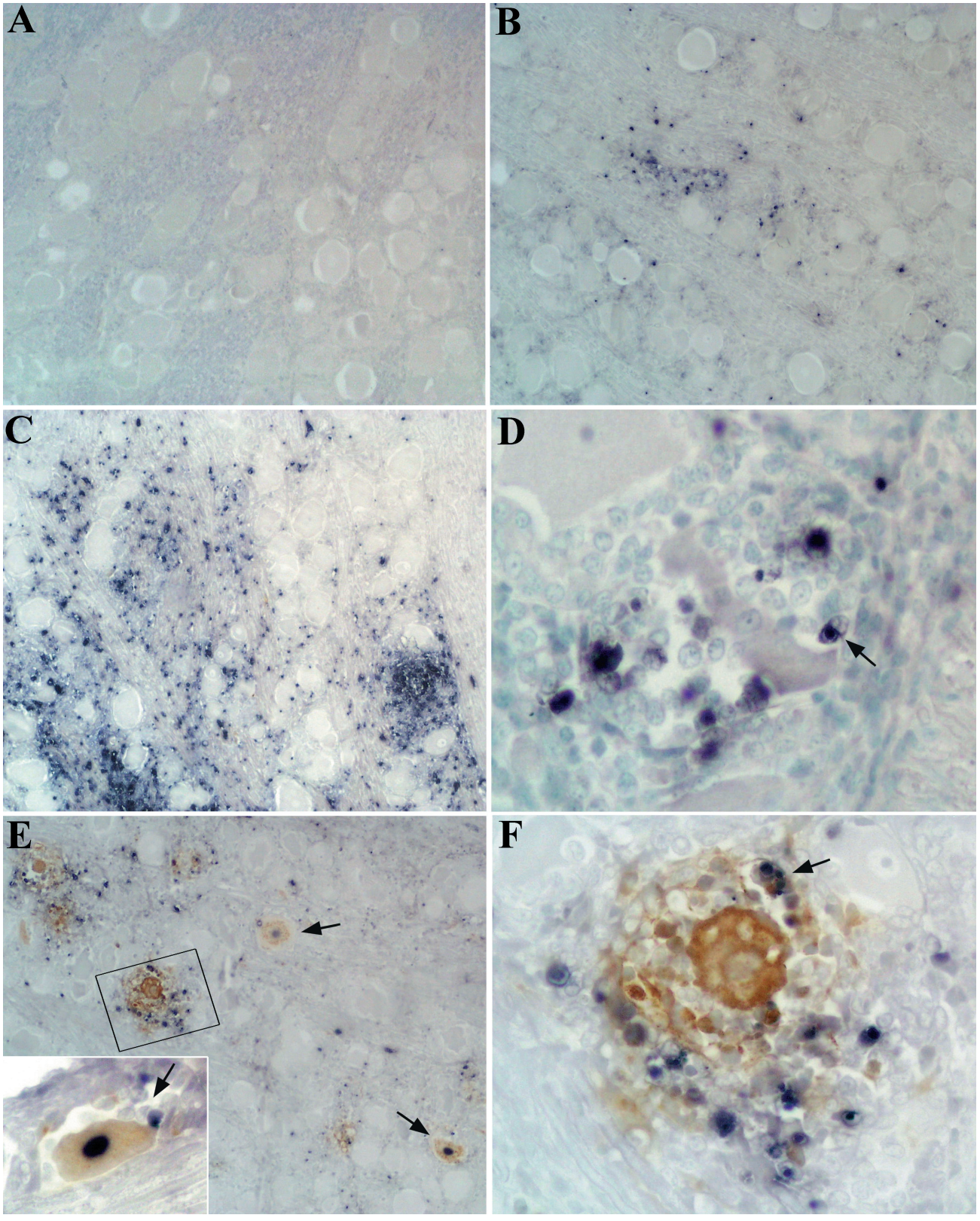

FIG. 3. Detection of apoptotic cells (A to D) by the in situ TUNEL method and colocalization of PRV antigen and apoptotic cells (E and F) by double labeling in the TG. (A) No apoptotic cells were detected in the TG at 12 hpi. (B) A few apoptotic inflammatory cells (black stain) were observed among infiltrating inflammatory cells at 24 hpi. (C) The maximum number of apoptotic cells was observed at 72 hpi. Note the absence of staining in neurons. (D) Apoptotic cells surrounding a neuron at 72 hpi. An apoptotic body seems to be phagocytosed by a macrophage (arrow). (E) PRV antigen (brown stain) and apoptotic cells (black stain) were distributed in the same regions of the TG. Three TUNEL-positive neurons (arrows and inset) were detected at 48 hpi. Note the presence of immune cells (arrow) in direct apposition to the IHC-positive–TUNEL-positive neuron shown in the inset. (F) Detail of boxed area in panel E under higher magnification. PRV-infected neurons were usually TUNEL negative. A double-labeled apoptotic cell can be identified (arrow). Original magnifications, ×100 (A, B, C, and E) and ×400 (D, F, and E [inset]).

for either viral antigen or apoptosis, but some colabeled cells were also detected (Fig. 3F). However, we also noticed a marked decrease in staining of PRV antigen in all sections tested for double labeling. Therefore, we cannot rule out the possibility that the relative number of double-labeled cells among infiltrating inflammatory cells is greater than observed.

Transmission electron microscopy. Analysis of thin sections confirmed that a number of mononuclear inflammatory cells found in the TG at 48 and 72 hpi exhibited typical ultrastructural features of apoptosis. Particularly, numerous infiltrating lymphocytes could be observed undergoing this type of cell death. Apoptotic lymphocytes were evidenced by the marked nuclear and cytoplasmic condensation, showing extremely compacted nuclear chromatin and the nucleus often fragmented into electron-dense masses (Fig. 4A and B). Apoptotic bodies, intact or in the process of being degraded within phagolysosomes, were frequently identified in the cytoplasm of macrophages (Fig. 4B) and occasionally in satellite cells (Fig. 4C). Consistent with our findings at the level of light microscopy, macrophages exhibiting morphological characteristics of apoptosis were occasionally observed. In addition to apoptosis, necrosis also occurred among infiltrating immune cells, since few necrotic macrophages were present within foci of inflammation (Fig. 4B). These necrotic cells displayed a swollen appearance, with dilation and marked dissolution of cytoplasmic organelles and rupture of the plasma membrane. Intranuclear or intracytoplasmic capsids were not observed in infiltrating macrophages or lymphocytes.

Neurons at early stages of infection showed complex invaginations of the nuclear envelope and margination of the nucleus to the periphery of the neuronal body. Cytoplasmic organelles remained almost intact, apart from a slight dilation of reticulum endoplasmic cisternae and Golgi profiles. In the connective tissue surrounding infected neurons, infiltrating inflammatory cells were usually present (Fig. 4A). Lymphocytes and macrophages were often localized within the enlarged spaces that became apparent between infected neurons and their surrounding satellite cells (Fig. 4B). Nucleocapsids were detected in the nucleus and cytoplasm of infected neurons, but they were not observed in the reactive satellite cells. Neurons at advanced stages of infection displayed profound pathological changes and were surrounded by large numbers of inflammatory cells (Fig. 4D). Their nuclei showed marked convolution of the nuclear envelope and margination of the chromatin against the inner nuclear membrane. Capsids at different stages of assembly were observed in the nucleoplasm, but identification of cytoplasmic nucleocapsids or even organelles was difficult due to the dense degeneration of this cell compartment. Most strikingly, we could observe a single infected sensory neuron that showed typical features of apoptosis at 72 hpi (Fig. 4E). These features consisted of nuclear chromatin condensation into an amorphous electron-dense mass and a compacted cytoplasm containing altered mitochondria and translucent vacuoles. Intracytoplasmic aggregations of empty capsids and DNA-containing nucleocapsids were evident (Fig. 4F and G), but enveloped nucleocapsids were not observed within the condensed cytoplasm.

DISCUSSION

In this study, we investigated the ability of a virulent strain of PRV to induce and block apoptosis in the TG during acute infection of swine. The findings reported here strongly suggest that PRV is able to inhibit apoptosis of TG neurons induced by the virus itself as well as by cytotoxic cells, although sporadic neuronal virus-induced apoptosis also occurs. Furthermore, our results also suggest that viral infection activates the cell death program both directly and indirectly in part of the inflammatory cells that infiltrate the TG.

TG tissue sections assayed simultaneously for the presence of PRV antigen by IHC and for apoptosis by TUNEL indicated that the majority of the infected neurons were not undergoing apoptosis. The implication of this finding is that PRV carries a gene(s) whose function is to inhibit apoptosis as a cellular response to viral infection. It is tempting to speculate about the identity of the gene products expressed by PRV with the capacity to interfere with elements of the highly controlled biochemical pathway which regulates cell death. The protein kinase encoded by the PRV Us3 gene and expressed during productive infection (42, 47) might have an antiapoptotic function in this virus, as it does in HSV-1 and HSV-2 (15, 21, 25). The PRV LAT gene is also a suitable candidate to play a role in blocking the host cell apoptotic response to viral infection, similar to HSV-1 and BHV-1 LAT genes (8, 34). In that respect, there is recent evidence that the PRV LAT gene is also transcribed during a productive infection of cultured cells and that one of the three lytic cycle viral RNAs expressed could be translated (22). Notably, the authors found that the putative protein encoded by open reading frame 1 of this RNA has homology to an inhibitor of apoptosis expressed in muscle cells (22). If the Us3 and LAT gene products retain antiapoptotic activity in PRV, they may be cooperating with themselves or with additional antiapoptotic gene products to prevent apoptosis of the infected neurons.

The failure to detect DNA fragmentation in most of the PRV-infected neurons is even more striking if we take into account that numerous mononuclear inflammatory cells were seen in direct apposition to them. Although immunocytochemical studies would be necessary in order to identify the various subclasses of infiltrating immune cells in the TG, it is expected that cytotoxic T lymphocytes and NK cells are present among them. These specialized immune cells destroy virus-infected cells, including neurons, by inducing apoptosis (5, 13, 20, 30). Thus, our findings suggest that PRV blocks not only the execution of the cell death program triggered as a direct response of the host cell to virus infection but also apoptosis induced by cytolytic cells during productive infection in its host. Similarly, it has been reported that HSV-1 protects infected cells from apoptosis induced by cytotoxic T lymphocytes (20) as well as by the effectors of the immune system, such as Fas and tumor necrosis factor alpha-mediated pathways (13).

However, we also detected the presence of a small number of IHC-positive–TUNEL-positive neurons in the TGs of one of the animals killed at 48 hpi. These cells displayed a well-preserved morphology, suggesting that they were recently infected neurons, and the associated inflammatory reaction was lower than that shown by IHC-positive–TUNEL-negative neurons. The detection of PRV antigen in the cytoplasm of these

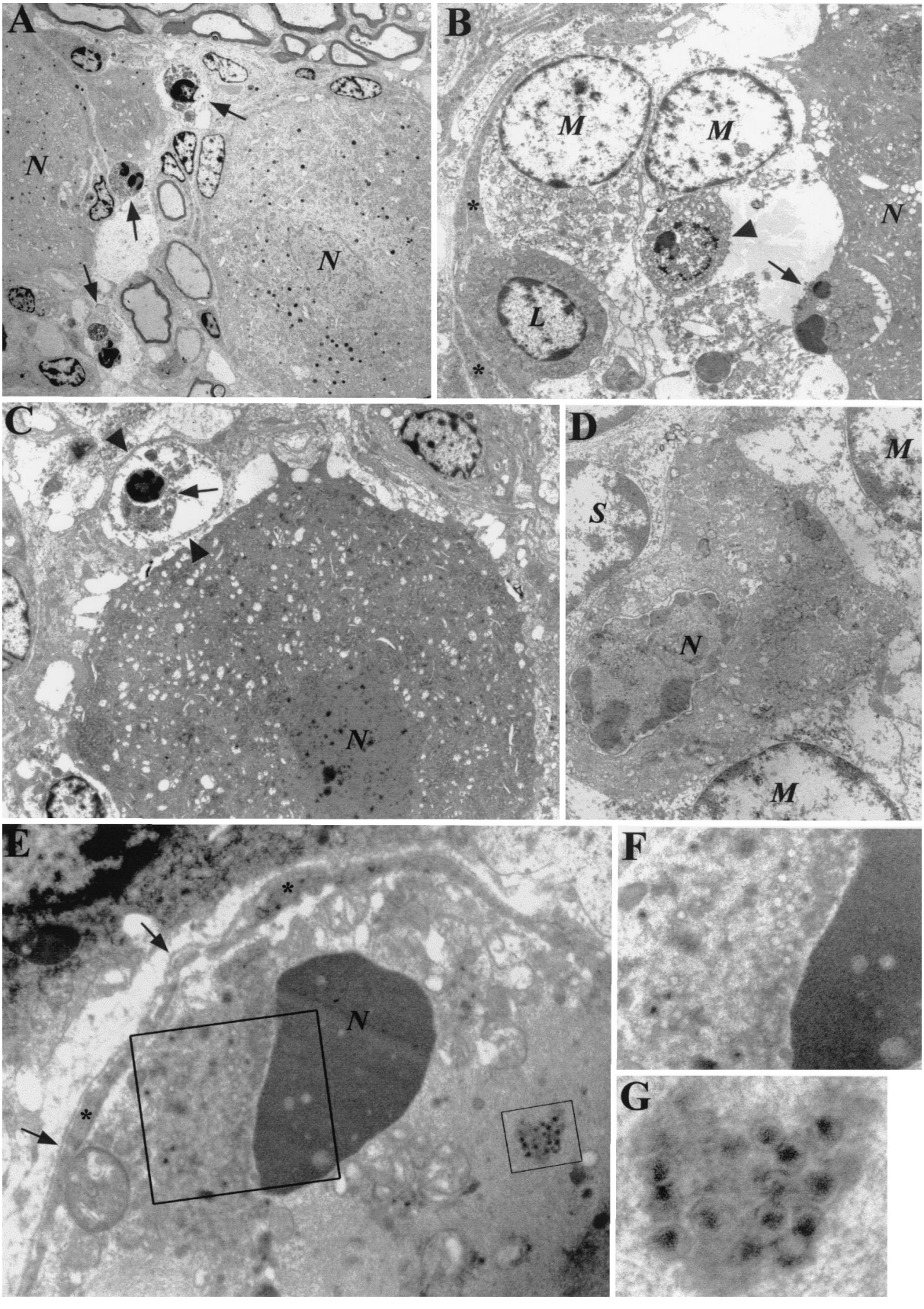
A
N
N
B
M
M
N
L
C
N
D
M
S
N
M
E
N
F
G

apoptotic neurons, together with the absence of neurons with an IHC-negative–TUNEL-positive phenotype, indicates that virus infection directly triggered the apoptotic pathway. Curiously enough, staining of PRV antigen in apoptotic neurons was lighter than staining in IHC-positive–TUNEL-negative neurons. It has been suggested that apoptotic cells display a reduced immunoreactivity due to extensive cell shrinkage and proteolysis of cytoplasmic proteins, thus hindering or precluding the recognition of antigenic sites (31).

Electron microscopy examination allowed us to identify one infected ganglionic neuron exhibiting morphological features of apoptosis in the TG of a pig killed at 72 hpi. This finding confirmed on the one hand that apoptotic neurons detected on paraffin sections were not false-positive results of the TUNEL method due to nonspecific DNA degradation during necrotic cell death and on the other hand that neuronal cell death was the result of virus infection. Naked capsids and nucleocapsids measuring approximately 100 nm in widest diameter were found in the cytoplasm of this neuron. Unlike the nuclei of the other PRV-infected neurons analyzed during this experiment, the nucleus of the apoptotic neuron contained condensed chromatin, a morphological hallmark of apoptosis (17, 46).

The presence of neuronal apoptosis in the TG of PRV-infected pigs was not unexpected, since apoptosis is an important strategy of cell defense against viral infections (32, 39, 41). PRV might have been unable to block the cell death pathway after virus-induced activation of apoptosis, so that the biochemical cascade leading to chromosomal DNA fragmentation was actually completed. Since few immune cells were also observed in direct apposition to apoptotic neurons, another possibility is that cytotoxic cells might have induced the execution of the cell death program before viral inhibition was effective. Finally, the low apoptosis level detected in PRV-infected neurons in this study is rather similar to that observed during acute infection in the rabbit TG with a wild-type strain of HSV-1 (34), indicating that this is a sporadic but not unusual event during productive infection of sensory TG neurons and probably of other types of neurons by alphaherpesviruses.

PRV infection of TG neurons induced the focal recruitment of numerous immune cells, mainly monocytes/macrophages and lymphocytes, which entered the infected regions from capillary vessels. The magnitude of the organized inflammatory reaction was temporally and spatially correlative to the extent of the infection and the appearance of lesions in the TG of the infected animals. Many lymphocytes and macrophages located around PRV-infected neurons were also infected, as was revealed by IHC and ISH assays.

Inflammatory cells exhibiting morphological characteristics of apoptosis were a common finding from 48 hpi until the end of the experiment. Almost all of the apoptotic cells were localized within foci of inflammation that were organized around neurons showing apparent pathological changes. The occurrence of apoptosis among infiltrating immune cells was subsequently corroborated by the TUNEL method and ultrastructural examination. The TUNEL method revealed the presence of apoptotic cells among infiltrating inflammatory cells even earlier, at 24 hpi. According to their size and morphological features, most apoptotic cells seemed to be lymphocytes and, to a low extent, macrophages. The question arising after this observation is whether the immune cells dying by apoptosis were also infected with PRV or whether apoptosis occurred in uninfected bystander cells which are near infected cells.

Although our double-labeling experiments showed that PRV antigen-positive cells and TUNEL-positive cells were concentrated in the same areas of the TG, the majority of the infiltrating inflammatory cells were labeled for either PRV antigen or apoptosis and only few cells were colabeled for both. However, colocalization of both positive signals on individual cells was difficult to perform, due to the smallness of the cells and to the scarce cytoplasm associated with the apoptotic signal. Therefore, it is possible that the relative number of infected apoptotic cells among immune cells is higher than observed. Moreover, there are several factors which would also confirm this supposition. (i) The ICH assay showed the presence of PRV antigen in the cytoplasm of larger numbers of apoptotic inflammatory cells. (ii) We noticed a marked decrease in staining of PRV antigen in the sections tested for double labeling, probably due to degradation of antigenic sites during protease digestion. (iii) Apoptotic neurons exhibited lighter staining of PRV antigen than did IHC-positive–TUNEL-negative neurons, suggesting that this is likely to occur in infiltrating immune cells as well. (iv) IHC-negative–TUNEL-positive infiltrating immune cells can be infected, but the amount of PRV antigen expressed in these cells may not be enough to be detected by IHC, or else a nonproductive infection may have taken place (28). (v) Apoptotic cells break into apoptotic bodies, some of which can be formed exclusively by portions of IHC-positive cytoplasm, while some others can hold TUNEL-positive nuclear fragments.

On the other hand, we cannot exclude the possibility that apoptosis observed among infiltrating inflammatory cells occurs in uninfected bystander cells present in the vicinity of PRV-infected cells. This indirect mechanism of virus-induced apoptosis has been proposed to occur during infection by var-

FIG. 4. Transmission electron microscopy of TG at 48 hpi (A) and 72 hpi (B to G). (A) Apoptotic lymphocytes (arrows) in the connective tissue between two neurons (*N*). (B) Inflammatory cells within the enlarged space between a neuron (*N*) and its satellite cells (asterisks). The macrophages (*M*) show morphological features of necrosis, and one of them contains a partially degraded lymphocyte within its cytoplasm (arrowhead). An apoptotic lymphocyte (arrow) with highly condensed nuclear fragments and a healthy lymphocyte (*L*) can also be identified. (C) A moderately degraded apoptotic lymphocyte (arrow) is surrounded by thin cytoplasmic projections (arrowheads) of a satellite cell, which indicates phagocytosis. An infected neuron (*N*) is shown. (D) A TG neuron (*N*) exhibiting advanced pathological changes is surrounded by a satellite cell (*S*) and two macrophages (*M*). The infected neuron shows margination of nuclear chromatin and convolution of the nuclear outline. (E) Apoptotic neuron displaying a condensed cytoplasm and a highly condensed nucleus (*N*). A surrounding satellite cell (asterisks) with its basal lamina (arrows) is displayed. (F and G) Details of boxed areas in panel E under higher magnification. (F) Empty and DNA-containing capsids measuring 100 nm in diameter in the cytoplasm of the apoptotic neuron. (G) Aggregate of naked nucleocapsids. The original negatives were digitized with a scanner (Epson GT-7000 photo), and brightness and contrast were corrected by using the graphic program Adobe Photoshop 4.0 for Windows. Original magnifications, ×1,000 (A), ×2,500 (B and D), ×4,000 (C), and ×10,000 (E).

ious viruses, such as human immunodeficiency virus type 1 (9, 16), reovirus (31), HSV-1 (19), and BHV-1 (44). The local release of immunologically active cytokines (tumor necrosis factor alpha, gamma interferon) from ganglionic cells and infiltrating immune cells can account for the presence of uninfected apoptotic cells near PRV-infected cells (31, 40). In addition, it has been reported that CD3/T-cell receptor molecular complex stimulation of activated T lymphocytes triggers apoptosis, an event termed activation-induced cell death and mediated by the Fas and tumor necrosis factor receptor pathways (3, 24, 45). Thus, activation-induced cell death could also be involved in the induction of apoptosis in uninfected lymphocytes during PRV infection of the TG. Finally, there is the possibility that the TUNEL technique may have detected nonspecifically degraded DNA fragments due to necrotic cell death, since few necrotic macrophages were observed within foci of inflammation.

Therefore, our results suggest that infection of the pig TG by PRV induces the death of infiltrating immune cells by a combination of direct and indirect mechanisms. However, it is also possible that apoptosis of immune cells is triggered mainly by a direct mechanism, but because of the difficulty in identifying infected apoptotic cells accurately, either TUNEL-positive or IHC-positive cells are detected more frequently than double-labeled cells.

It has been shown that both HSV-1 and BHV-1 can infect activated T lymphocytes, leading to apoptosis of infected cells (12, 14, 19, 38, 44). One of the hypotheses put forward is that uninfected cytotoxic T lymphocytes recognize and kill infected T lymphocytes. This results in an immune evasion mechanism which can be used by viruses able to infect and replicate in activated T lymphocytes, even though these viruses mainly propagate in nonlymphoid cells (38). Regarding PRV, it is known that it infects monocytes and activated T lymphocytes, although viral replication in these cells is clearly restricted (28). The death of some infected monocytes and lymphocytes has also been reported after an in vitro inoculation with PRV (7, 43), but the precise mechanisms of cell death were not investigated. The results of our in vivo study show the occurrence of PRV-induced apoptosis in mononuclear immune cells that infiltrate the TG and suggest that it may account for suppression of cell-mediated immunity following infection of swine.

The results obtained in this study provide new and significant data on the interactions between PRV and its natural host, which can contribute to a better understanding of the pathogenesis of PRV infection. In summary, a virulent strain of PRV is able to inhibit apoptosis of the majority of infected TG neurons during acute infection of swine. PRV inhibition of apoptosis allows the production of high yields of progeny virus which can spread transsynaptically and infect higher-order neuronal levels in the CNS. Significantly, the ability of PRV to block apoptosis of infected neurons may play an important role in the establishment, maintenance, and reactivation of latent infections in the TG of infected pigs. PRV also seems to have developed an efficient strategy of evasion against cell-mediated immunity: on the one hand, most PRV-infected TG neurons are protected from cytotoxic cell-induced apoptosis; on the other hand, the role of immune cells in controlling PRV infection in the TG is impaired, since many of the cells recruited into the infected areas die via induction of apoptosis.

ACKNOWLEDGMENTS

We thank E. Puentes (CZ Veterinaria, S. L., Pontevedra, Spain) for providing the PRV strain E-974, M. B. Pensaert (University of Ghent, Ghent, Belgium) for providing the anti-PRV antibody, and F. A. Osorio (University of Nebraska, Lincoln) for providing the PRV plasmid.

This work was supported by a research grant from the Xunta de Galicia (XUGA26105B98).

REFERENCES

1. **Aubert, M., and J. A. Blaho.** 1999. The herpes simplex virus type 1 regulatory protein ICP27 is required for the prevention of apoptosis in infected human cells. J. Virol. **73:**2803–2813.
2. **Aubert, M., J. O'Toole, and J. A. Blaho.** 1999. Induction and prevention of apoptosis in human HEp-2 cells by herpes simplex virus type 1. J. Virol. **73:**10359–10370.
3. **Ayroldi, E., O. Zollo, L. Cannarile, F. D'Adamio, U. Grohmann, D. V. Delfino, and C. Riccardi.** 1998. Interleukin-6 (IL-6) prevents activation-induced cell death: IL-2-independent inhibition of Fas/fasL expression and cell death. Blood **92:**4212–4219.
4. **Balasch, M., J. Pujols, J. Segalés, J. Plana-Durán, and M. Pumarola.** 1998. Study of the persistence of Aujeszky's disease (pseudorabies) virus in peripheral blood mononuclear cells and tissues of experimentally infected pigs. Vet. Microbiol. **62:**171–183.
5. **Berke, G.** 1995. The CTL's kiss of death. Cell **81:**9–12.
6. **Card, J. P., and L. W. Enquist.** 1995. Neurovirulence of pseudorabies virus. Crit. Rev. Neurobiol. **9:**137–162.
7. **Chinsakchai, S., and T. W. Molitor.** 1992. Replication and immunosuppressive effects of pseudorabies on swine peripheral blood mononuclear cells. Vet. Immunol. Immunopathol. **30:**247–260.
8. **Ciacci-Zanella, J., M. Stone, G. Henderson, and C. Jones.** 1999. The latency-related gene of bovine herpesvirus 1 inhibits programmed cell death. J. Virol. **73:**9734–9740.
9. **Cicala, C., J. Arthos, A. Rubbert, S. Selig, K. Wildt, O. J. Cohen, and A. S. Fauci.** 2000. HIV-1 envelope induces activation of caspase-3 and cleavage of focal adhesion kinase in primary human $CD4^+$ T cells. Proc. Natl. Acad. Sci. USA **97:**1178–1183.
10. **Enquist, L. W.** 1994. Infection of the mammalian nervous system by pseudorabies virus (PRV). Semin. Virol. **5:**221–231.
11. **Enquist, L. W., P. J. Husak, B. W. Banfield, and G. A. Smith.** 1999. Infection and spread of alphaherpesviruses in the nervous system. Adv. Virus Res. **51:**237–347.
12. **Eskra, L., and G. A. Splitter.** 1997. Bovine herpesvirus-1 infects activated $CD4^+$ lymphocytes. J. Gen. Virol. **78:**2159–2166.
13. **Galvan, V., and B. Roizman.** 1998. Herpes simplex virus 1 induces and blocks apoptosis at multiple steps during infection and protects cells from exogenous inducers in a cell-type-dependent manner. Proc. Natl. Acad. Sci. USA **95:**3931–3936.
14. **Griebel, P. J., H. B. Ohmann, M. J. P. Lawman, and L. A. Babiuk.** 1990. The interaction between bovine herpesvirus type 1 and activated bovine T lymphocytes. J. Gen. Virol. **71:**369–377.
15. **Hata, S., A. H. Koyama, H. Shiota, A. Adachi, F. Goshima, and Y. Nishiyama.** 1999. Antiapoptotic activity of herpes simplex virus type 2: the role of Us3 protein kinase gene. Microbes Infect. **1:**601–607.
16. **Herbein, G., C. van Lint, J. L. Lovett, and E. Verdin.** 1998. Distinct mechanisms trigger apoptosis in human immunodeficiency virus type 1-infected and in uninfected bystander T lymphocytes. J. Virol. **72:**660–667.
17. **Huppertz, B., H.-G. Frank, and P. Kaufmann.** 1999. The apoptosis cascade—morphological and immunohistochemical methods for its visualization. Anat. Embryol. **200:**1–8.
18. **Iglesias, G. J., M. Trujano, J. Lokensgard, and T. Molitor.** 1992. Study of the potential involvement of pseudorabies virus in swine respiratory disease. Can. J. Vet. Res. **56:**74–77.
19. **Ito, M., M. Watanabe, H. Kamiya, and M. Sakurai.** 1997. Herpes simplex virus type 1 induces apoptosis in peripheral blood T lymphocytes. J. Infect. Dis. **175:**1220–1224.
20. **Jerome, K. R., J. F. Tait, D. M. Koelle, and L. Corey.** 1998. Herpes simplex virus type 1 renders infected cells resistant to cytotoxic T-lymphocyte-induced apoptosis. J. Virol. **72:**436–441.
21. **Jerome, K. R., R. Fox, Z. Chen, A. E. Sears, H.-Y. Lee, and L. Corey.** 1999. Herpes simplex virus inhibits apoptosis through the action of two genes, Us5 and Us3. J. Virol. **73:**8950–8957.
22. **Jin, L., and G. Scherba.** 1999. Expression of the pseudorabies virus latency-associated transcript gene during productive infection of cultured cells. J. Virol. **73:**9781–9788.
23. **Jones, C.** 1999. Alphaherpesvirus latency: its role in disease and survival of the virus in nature. Adv. Virus Res. **51:**81–133.
24. **Kabelitz, D., and O. Janssen.** 1997. Antigen-induced death of T-lymphocytes. Front. Biosci. **2:**61–77.
25. **Leopardi, R., C. Van Sant, and B. Roizman.** 1997. The herpes simplex virus 1 protein kinase Us3 is required for protection from apoptosis induced by the

virus. Proc. Natl. Acad. Sci. USA **94:**7891–7896.
26. **Mulder, W. A. M., L. Jacobs, J. Priem, G. L. Kok, F. Wagenaar, T. G. Kimman, and J. M. A. Pol.** 1994. Glycoprotein gE-negative pseudorabies virus has a reduced capability to infect second- and third-order neurons of the olfactory and trigeminal routes in the porcine central nervous system. J. Gen. Virol. **75:**3095–3106.
27. **Nauwynck, H., and M. B. Pensaert.** 1992. Abortion induced by cell-associated pseudorabies virus in vaccinated sows. Am. J. Vet. Res. **53:**489–493.
28. **Nauwynck, H., and M. B. Pensaert.** 1994. Virus production and viral antigen expression in porcine blood monocytes inoculated with pseudorabies virus. Arch. Virol. **137:**69–79.
29. **Nauwynck, H., and M. B. Pensaert.** 1995. Cell-free and cell-associated viremia in pigs after oronasal infection with Aujeszky's disease virus. Vet. Microbiol. **43:**307–314.
30. **Nishioka, W. K., and R. M. Welsh.** 1994. Susceptibility to cytotoxic T lymphocyte-induced apoptosis is a function of the proliferative status of the target. J. Exp. Med. **179:**769–774.
31. **Oberhaus, S. M., R. L. Smith, G. H. Clayton, T. S. Dermody, and K. L. Tyler.** 1997. Reovirus infection and tissue injury in the mouse central nervous system are associated with apoptosis. J. Virol. **71:**2100–2106.
32. **O'Brien, V.** 1998. Viruses and apoptosis. J. Gen. Virol. **79:**1833–1845.
33. **Page, G. R., F.-I. Wang, and E. C. Hahn.** 1992. Interactions of Aujeszky's disease virus with porcine peripheral blood lymphocytes. J. Leukoc. Biol. **52:**441–448.
34. **Perng, G.-C., C. Jones, J. Ciacci-Zanella, M. Stone, G. Henderson, A. Yukht, S. M. Slanina, F. M. Hofman, H. Ghiasi, A. B. Nesburn, and S. L. Wechsler.** 2000. Virus-induced neuronal apoptosis blocked by the herpes simplex virus latency-associated transcript. Science **287:**1500–1503.
35. **Posavad, C. M., J. J. Newton, and K. L. Rosenthal.** 1994. Infection and inhibition of human cytotoxic T lymphocytes by herpes simplex virus. J. Virol. **68:**4072–4074.
36. **Puentes, E., E. Cancio, A. Eiras, M. V. Nores, A. Aguilera, B. J. Regueiro, and R. Seoane.** 1993. Efficacy of various non-oily adjuvants in immunization against the Aujeszky's disease (pseudorabies) virus. J. Med. Vet. Ser. B **40:**353–365.
37. **Quiroga, M. I., J. M. Nieto, J. Sur, and F. Osorio.** 1998. Diagnosis of Aujeszky's disease virus infection in dogs by use of immunohistochemistry and in-situ hybridization. J. Vet. Med. Ser. A **45:**75–81.
38. **Raftery, M. J., C. K. Behrens, A. Muller, P. H. Krammer, H. Walczak, and G. Schonrich.** 1999. Herpes simplex virus type 1 infection in activated cytotoxic T cells: induction of fratricide as a mechanism of viral immune evasion. J. Exp. Med. **190:**1103–1113.
39. **Shen, Y., and T. E. Shenk.** 1995. Viruses and apoptosis. Curr. Opin. Genet. Dev. **5:**105–111.
40. **Shimeld, C., J. L. Whiteland, N. A. Willians, D. L. Easty, and T. J. Hill.** 1997. Cytokine production in the nervous system of mice during acute and latent infection with herpes simplex virus type 1. J. Gen. Virol. **78:**3317–3325.
41. **Teodoro, J. G., and P. E. Branton.** 1997. Regulation of apoptosis by viral gene products. J. Virol. **71:**1739–1746.
42. **van Zijl, M., H. van der Gulden, N. de Wind, A. Gielkens, and A. Berns.** 1990. Identification of two genes in the unique short region of pseudorabies virus; comparison with herpes simplex virus and varicella-zoster virus. J. Gen. Virol. **71:**1747–1755.
43. **Wang, F.-I., V. F. Pang, and E. C. Hahn.** 1988. Flow cytometric analysis of porcine peripheral blood leukocytes infected with pseudorabies virus. J. Leukoc. Biol. **43:**256–264.
44. **Winkler, M. T. C., A. Doster, and C. Jones.** 1999. Bovine herpesvirus 1 can infect $CD4^+$ T lymphocytes and induce programmed cell death during acute infection of cattle. J. Virol. **73:**8657–8668.
45. **Winoto, A.** 1997. Cell death in the regulation of immune responses. Curr. Opin. Immunol. **9:**365–370.
46. **Wyllie, A. H.** 1997. Apoptosis: an overview. Br. Med. Bull. **53:**451–465.
47. **Zhang, G., R. Stevens, and D. P. Leader.** 1990. The protein kinase encoded in the short unique region of pseudorabies virus: description of the gene and identification of its product in virions and in infected cells. J. Gen. Virol. **71:**1757–1765.